Available online at www.sciencedirect.com

ScienceDirect

Procedia Structural Integrity 2 (2016) 1221–1228

Structural Integrity Procedia

www.elsevier.com/locate/procedia

21st European Conference on Fracture, ECF21, 20-24 June 2016, Catania, Italy

Theoretical Approach for Developing the Thermographic Method in Ultrasonic Fatigue

V. Crupi[b], E. Guglielmino[b], O. Plekhov[a]*, A. Prokhorov[a], G. Risitano[b]

[a]*ICMM UB RAS, 1 Ak. Koroleva str., 614014 Perm, Russia*
[b]*University of Messina, Engineering Department, Contrada Di Dio (S. Agata), 98166 Messina, Italy*

Abstract

In the last years, several approaches were developed in literature for predicting the fatigue strength of different kinds of materials. One approach is the Thermographic Method, based on the thermographic technique. This study is devoted to the development of a theoretical approach for modeling of surface and undersurface fatigue crack initiation and temperature evolution during ultrasonic fatigue test. The proposed model is based on the statistical description of mesodefect ensemble and describes an energy balance in materials (including power of energy dissipation) under cyclic loading. The model allows us to simulate the damage to fracture transition and corresponding temperature evolution in critical cross section of a sample tested in very high cyclic fatigue regime.

Keywords: infrared thermography; self-heating test; gigacyclic fatigue regime; very high cycle fatigue; Thermographic Method

1. Introduction

It is well known that the metals have a complex structure, which is a hierarchy of different levels. Under deformation process, the structural evolution, observed at all scale levels, leads to irreversible deformation and failure. Under gigacyclic fatigue loading, such structural evolution goes under stress amplitude less than the yield stress of materials and fracture occurs under macroscopic “pure” elastic conditions. One of most critical issue of the gigacyclic fatigue is the location of fatigue crack initiation. The decreasing of stress amplitude leads to the

* Corresponding author. Tel.:+7-342-237-8321; fax: +7-342-237-8487.
E-mail address: poa@icmm.ru

10.1016/j.prostr.2016.06.156

shift of crack initiation from specimen surface to the bulk. The simulation of damage to fracture transition and corresponding temperature evolution allows one to use the Thermographic Method for predicting the fatigue strength.

Gigacyclic fatigue tests with a number of loading cycles of 10^8-10^{10} are generally performed on the ultrasonic fatigue testing machine. The initial fatigue tests were carried out in the symmetrical pull-push loading regime by Murakami at al. (1999), Bathias et al. (2004), Zhu at al. (2006). More recently, the experimental setups were modified to study the fatigue behavior under non zero mean stress by Liu et al. (2015) and under torsion loading by Mayer et al. (2015) and by Nikitin et al. (2016). The thermographic technique under gigcyclic fatigue test was used by Ranc et al. (2015), Plekhov et al. (2015) and Crupi et al. (2015), who developed the traditional Thermographic Method in order to extent it in very high cycle fatigue regime.

To develop a model of defect evolution under small stress amplitude, we have to choice the basic physical level of description of the material microstructure and describe the geometry of the elementary defects. One of the possible descriptions of defect kinetics is the statistical model of defect ensample. This model has to take into account the stochastically properties of defect initiation, their nonlinear integration and link between micropalsticity and damage accumulation. This work is devoted to the development of such model describing the damage to fracture transition and corresponding temperature evolution in the application to ultrasonic fatigue of metals.

As experimental basis, the paper includes an investigation of dilatation of Armco-iron samples and description of experimental attempts to develop an experimental technique for real time monitoring of the process accompanying damage evolution and damage to fracture transition in metals under ultrasonic fatigue. The study of mechanical properties was carried out based on the acoustic resonance method using a piezoelectric vibrator with the longitudinal oscillations at frequencies of about 100 kHz. The porosity of the samples was studied by the method of hydrostatic weighing.

2. Experimental investigation of dilatation evolution under ultrasonic fatigue test

2.1. A posteriori study of dilatation evolution and elastic properties degradation

Armco iron samples were used in our investigation. The fatigue tests were carried out using the Shimadzu USF-2000 ultrasonic testing machine, which provides the accelerated testing of the fatigue properties of materials at 20 kHz. The vibration generated by the piezo element is amplified by the booster and the horn and transmitted to the sample to generate repeated stress. In the ultrasonic fatigue testing system, the vibration system is constructed so that the longitudinal waves transmitted through the solid body are resonating. Consequently, stationary longitudinal waves are formed inside the vibration system (sample, horn and booster).

All the samples were tested at the constant stress amplitude up to the failure. The cooling of the sample was realized by an air stream.

The Young`s modulus E (a characteristic of elastic properties) and amplitude independent decrement δ (a characteristic of reversible micro plasticity properties) were determined using acoustic resonance method. The main peculiarity of the acoustic experiments is the small stress amplitude which doesn't change the dislocation density in the sample.

The measurements were carried out using sectional piezoelectric resonant vibrator. The longitudinal vibrations of samples have a frequency of about 100 kHz. The amplitude was varied in a wide range to investigate both a linear (amplitude-independent) and nonlinear (microplastic) areas.

Dilatation of samples was investigated using the method of hydrostatic weighing. The method involves weighing the specimen in air and in liquid (distilled water) at a constant temperature, as well as the determination of the density of the liquid used. Analytical balances AUW-120D Shimadzu was used for the experiments. The relative error of determining the density didn't exceed $2\ 10^{-4}$ g. The accuracy of the measurement of water temperature was 0.05°C.

The structural investigation techniques lead to changes in the shape and size of the investigated sample. As a result, we cannot use one and the same sample to study the structure evolution at different stages of loading. To solve this problem, we tested three samples from one sample series up to a specified number of loading cycles

and then subjected them to structural analysis. Sample 1 is initial state; sample 2 is relative to 9,01 10^8 cycles of loading at stress amplitude 161 MPa; sample 3 is relative to 2,1 10^9 cycles of loading at stress amplitude 161 MPa. The table 1 presents the geometry, weight, density, Young`s modulus and decrement of an iron at different stage of fatigue experiment and the evolution of these parameters versus length and diameter of samples.

The analysis of data presented in table 1 allows us to conclude that the increase of the number of cycles leads to the decrease of the sample density and the decrease of diameters leads to the increase of the dilation of the samples. It means that the dilatation can be considered as a measure of current damage state of a material. There is a considerable decrease of Young`s modulus with the increase of the number of cycles.

Table 1. Physical and geometrical parameters of samples with different diameters

Sample	m, g	d, mm	ρ, g/cm3	E, GPa	δ_i, 10^{-5}
Sample 1	4.65219	5.00	7.8787	186.2	63.0
	4.68840	5.00	7.8717	184.2	52.4
Sample2	4.43544	4.90	7.8708	182.5	47.1
	3.26927	4.22	7.8686	180.0	50.9
	4.63726	5.00	7.8640	184.4	52.5
Sample3	4.45456	4.90	7.8608	182.7	59.0
	3.26388	4.22	7.8602	181.7	68.4

2.2. In-situ monitoring of physical properties evolution under ultrasonic fatigue test

In the magnetic method, the ferromagnetic properties of the material is used to monitor processes that accompany the evolution of the material structure. This technique is a modification of the non-destructive ferroprobe testing method. In this case, the sample is simultaneously the object of study and the core of a ferroprobe. In this method, the parameter to be measured is magnetic permeability, because it changes at the time of defect nucleation.

During the experiment, two electromagnetic coils (magnetizing and measuring) were placed on the sample. The alternating current in the magnetizing coil magnetized the sample to saturation. This point was fixed by the appearance of the nonlinear useful signal in the measuring coil. It was found that the second harmonic of the measuring coil signal was most sensitive to the magnetic field variation inside the sample (inductance of sample).

To switch the magnetizing coil, a mini amplifier of signals was assembled based on the TDA2030a chip. The magnetizing coil can operate in two modes: stabilization of voltage and stabilization of current. The analog-digital convertor (ADC) NI is used to register the measuring coil signals. The instrument accuracy of the measurement voltage by ADC is 6 uV. The measurement data is analyzed in real time using the LabVIEW software package. A typical graph of the second harmonic amplitude of the measuring solenoid during the experiment is shown in the figure 1. The amplitude of the second harmonic increases significantly as a result of the magnetic saturation of the specimen due to changes in the magnetic permeability before specimen fracture.

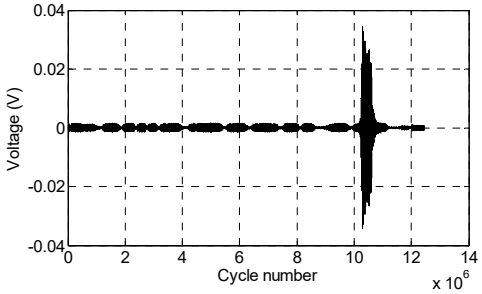

Fig. 1. The change of the second harmonic amplitude of the electric voltage on the measurement solenoid during fatigue test

3. Theoretical description of mesodefect ensemble evolution

The data obtained from studies of dilatation evolution shows that the volume defects play the important role in considering deformation process. These defects emerge at the early stage of deformation and effect on the microplasticity and failure processes. The value, geometrically representing the real microcracks with allowance made for a variety of their shapes, sizes and arbitrary orientations as well as or the crack initiated material loosening, can be introduced in terms of the dislocation theory. The dislocation loop D, bounding the surface S, where the displacement vector undergoes a finite increment equal the Burgers vector b, is characterized by the tensor of the dislocation moment $S\nu_i b_k$. The sum of N dislocation loops, which is equivalent to a microcrack, introduces the tensor of dislocation moment of a microcrack:

$$s_{ik} = \sum_{l=1}^{N} S^l \nu_i^l b_k^l, \tag{1}$$

where ν^l is the vector of a normal to the surface S of the 1-th loop. Small sizes and multiple character of microcrack nucleation as well as size and orientation distributions of microcracks permit averaging of their parameters over elementary volume to obtain the macroscopic tensor

$$p_{ik} = n\langle s_{ik} \rangle, \tag{2}$$

where n is a concentration of microcracks.

A solution of equation (2) in mean field approximation was proposed by Naimark et al. (2003). The solution depends on structural parameter δ and defect concentration n. To describe a real deformation process which characterized by the growth of defect concentration we propose that the representative material volume V_r contains $n_0 V_r$ defects nucleuses. Following Doudard et al. (2005) we propose that the applied stress activates the defects and this process can be described as a stochastic Poisson point process with intensity function $n(\Sigma)$.

Intensity function describes both the growth of active defects (which contribute to the defect induced strain) and growth defect nucleuses. Following the experimental data about evolution of microcrack concentration we can assume the following approximation for intensity function

$$n(\Sigma) = \frac{\alpha_0}{2}\left(1 + Erf\left(\frac{\Sigma - \Sigma_0}{\Sigma_1}\right)\right)(n_0 + \alpha_1 \Sigma), \tag{3}$$

where $\alpha_0, \alpha_1, \Sigma_0, \Sigma_1$ - material constants.

The probability of find N active defects in representative material volume is $P(N) = \frac{n(\Sigma)^N Exp(-n(\Sigma))}{N!}$

The stochastic consideration of defect evolution process changes the self-consistency equation (2). For small stress values we obtain a pure elasticity which passes to the plastic deformation with different intensity. The intensity of plastic deformation and damage accumulation depends on the initial concentration of defect nucleuses.

A thermomechanical process of plastic deformation obeys the momentum balance equation and the first and second laws of thermodynamics. In the case of small deformation, these equations involve the following thermodynamic quantities: density ρ, specific internal energy e, strain and stress tensors ε_{ik} and σ_{ik}, heat supply r, heat flux vector q, specific Helmholtz free energy F, and specific entropy η. The energy balance and the entropy can be written as

$$\dot{e} \equiv \left(\dot{F} + \eta\dot{T} + \dot{\eta}T\right) = \frac{1}{\rho}\sigma_{ik} : \dot{\varepsilon}_{ik} + r - \overline{\nabla} \cdot \overline{q}\,; \quad \dot{\eta} - \overline{\nabla} \cdot \left(\frac{\overline{q}}{T}\right) - r' \geq 0, \tag{4}$$

where the superposed dot stands for the material time derivative.

We assume the following kinematical relationship for the material under study

$$\widetilde{\varepsilon} = \widetilde{\varepsilon}^{\,e} + \widetilde{\varepsilon}^{\,p} + \widetilde{p} + \widetilde{\beta}(T - T'), \tag{5}$$

where $\widetilde{\varepsilon}^{\,e}$ is the elastic strain tensor, $\widetilde{\varepsilon}^{\,p}$ is the plastic strain tensor (related to the defect motion), $\widetilde{\beta}$ is the thermal expansion coefficient tensor, and T' is the reference temperature.

To introduce the list of independent variables for the free energy $F\left(\widetilde{\varepsilon}^{\,e}, T, \widetilde{p}\right)$ the equations (4) give

$$-\vec{q}\cdot\frac{\overline{\nabla}T}{T}-F_{\tilde{p}}:\dot{\tilde{p}}+\frac{1}{\rho}\tilde{\sigma}:\left(\dot{\tilde{\varepsilon}}^{p}+\dot{\tilde{p}}\right)\geq 0, \tag{6}$$

$$c\dot{T}=\overline{\nabla}\overline{q}+r+Q^{e}+Q^{p}, \tag{7}$$

where $Q^{e}=TF_{T\tilde{\varepsilon}^{e}}:\dot{\tilde{\varepsilon}}^{e}$ - heat production due to thermoelastic effect; $Q^{p}=\frac{1}{\rho}\tilde{\sigma}:\dot{\tilde{\varepsilon}}^{p}+\left(\frac{1}{\rho}\tilde{\sigma}-F_{p}\right):\dot{\tilde{p}}$ - represents the inelastic part to the heat production; c - the specific heat capacity.

To assume the linear links between thermodynamic forces and the thermodynamics fluxes, we obtain the constitutive equations

$$\dot{\tilde{\varepsilon}}^{p}=l_{\varepsilon^{p}}F_{\tilde{\varepsilon}^{e}}+l_{\varepsilon^{p}p}\left(F_{\tilde{\varepsilon}^{e}}-F_{\tilde{p}}\right), \tag{8}$$

$$\dot{\tilde{p}}=l_{p}\left(F_{\tilde{\varepsilon}^{e}}-F_{\tilde{p}}\right)+l_{\varepsilon^{p}p}F_{\tilde{\varepsilon}^{e}}, \tag{9}$$

where the function F_{p} follows from the presentation of free energy given by the statistical model of solid with mesodefects.

To consider the influence of diffusion processes on defect nucleation and evolution and to study the localization effects of the damage accumulation, we have introduced in the expression of the total free energy F the term describing spatially-nonuniform distribution of microcrack density tensor p_{ik}

$$\mathrm{F}=\frac{1}{2}K\varepsilon_{ll}^{e\,2}+\mu\left(\varepsilon_{ik}^{e}-\frac{1}{3}\varepsilon_{ll}^{e}\delta_{ik}\right)^{2}+F\left(p_{ik}\right)+\frac{1}{2}\kappa\left(\frac{\partial p_{ik}}{\partial r}\right)^{2}. \tag{10}$$

In order to evaluate tensor F_{p}, we have to consider the equation (11) as a functional determined for a representative material volume. For one dimension problem we can write

$$F_{p}=\frac{\delta\mathrm{F}}{\delta p_{ik}}=\frac{\partial\mathrm{F}}{\partial p_{ik}}-\frac{\partial}{\partial x_{l}}\left[\frac{\partial\mathrm{F}}{\partial\left(\partial p_{ik}/\partial x_{l}\right)}\right]. \tag{11}$$

The system (8)–(9) in the case of uniaxial cyclic loading ($\sigma_{zz}=\sigma$, $e_{zz}=e$, $p_{zz}=p$) takes the form

$$\dot{\varepsilon}^{p}=l_{\varepsilon^{p}}\sigma+l_{\varepsilon^{p}p}\left(\sigma-\frac{\partial F}{\partial p}-\frac{\partial}{\partial x}D\frac{\partial p}{\partial x}\right), \tag{12}$$

$$\dot{p}=l_{p}\left(\sigma-\frac{\partial F}{\partial p}-\frac{\partial}{\partial x}D\frac{\partial p}{\partial x}\right)+l_{\varepsilon^{p}p}\sigma, \tag{13}$$

where D is the coefficient of self-diffusion.

4. Numerical simulation of damage to fracture transition and temperature distribution (surface and subsurface fatigue crack initiation)

To describe the bulk defect (pores, microcracks) evolution specimen we will consider a one component of defect induced strain. Under high cyclic and gigacyclic fatigue we can propose a weak interaction of defect accumulation and microplastisity processes and write the equations (12),(13) as follows ($l_{\varepsilon^{p}p}->0$)

$$\dot{p}_{zz}=l_{p}\left(\sigma_{zz}-\frac{\partial F}{\partial p_{zz}}+\frac{\partial}{\partial x_{i}}D\frac{\partial p_{zz}}{\partial x_{i}}\right). \tag{14}$$

To describe the defect evolution in critical cross-section of the sample tested in ultrasonic testing machine let write the equation (14) in cylindrical coordinates r,φ:

$$\dot{p}_{zz}=l_{p}\left(\sigma_{zz}-\frac{\partial F}{\partial p_{zz}}+D\left(\frac{\partial p_{zz}}{\partial r}\right)^{2}+D\left(\frac{\partial p_{zz}}{\partial\varphi}\right)^{2}+Dp_{zz}\left(\frac{\partial^{2}p_{zz}}{\partial r^{2}}\right)+D\frac{p_{zz}}{r}\left(\frac{\partial p_{zz}}{\partial r}\right)+D\frac{p_{zz}}{r^{2}}\left(\frac{\partial^{2}p_{zz}}{\partial\varphi^{2}}\right)\right).$$

We can used the following boundary conditions

$$D\frac{\partial p}{\partial r}\bigg|_{r=R} = -h\left(p_{zz} - p_0\right), \tag{15}$$

where h the constant which determine the boundary conditions.

The equation (14) requests an approximation of function $\sigma - \partial F/\partial p$ which determined the equilibrium states of materials with defects. Taking into account the solution of statistical problem we can propose the following approximation for defect evolution law

$$\sigma_{zz} - \frac{\partial F}{\partial p_{zz}} = n a_0 {\sigma_{zz}}^2 \left(p_{zz} + p_0\right)^2 - a\, p_{zz}, \tag{16}$$

where n is initial defect concentration, σ is stress, p_0, a_0, a are materials constants.

To explain the different mechanisms of crack initiation on specimen surface and in the bulk we have to consider a surface as a physical object with high concentration of incomplete atomic planes and other defect of different nature. As a result we can consider the surface as negative source with infinite capacity which has a great influence on the defect evolution. This influence can be described by the value of constant h in the boundary condition (15). There are two limiting cases for equation (15). The first case is $h \to \infty \Rightarrow p\big|_{p\in S} = 0$. It means the surface is the sink of infinite capacity. The second case is $h \to 0 \Rightarrow D\frac{\partial p}{\partial x}\Big|_{p\in S} = 0$. The surface is closed for the defect diffusion.

To describe the temperature evolution we have to consider the equation (7). If we propose a weak effect of elastic and plastic deformation on dissipation it can be rewritten as follows

$$\rho c\dot{T} = (\sigma_{zz} - \frac{\partial F}{\partial p_{zz}})\dot{p}_{zz} + \lambda\left(\frac{\partial^2 T}{\partial r^2}\right) + \frac{\lambda}{r}\left(\frac{\partial T}{\partial r}\right) + \frac{\lambda}{r^2}\left(\frac{\partial^2 T}{\partial \varphi^2}\right) \tag{17}$$

Using following dimensionless variables $\tau = t\, l_p a$, $\Psi = \sigma\sqrt{\frac{a_0}{a}}$, $n' = \frac{n}{n_0}$, $r' = r/R$ the problem can be written in form

$$\dot{p}_{zz} = n'\Psi^2(p_{zz} + p_0)^2 - p_{zz} + \left(D'\left(\frac{\partial p_{zz}}{\partial r}\right)^2 + D'\left(\frac{\partial p_{zz}}{\partial \varphi}\right)^2 + D' p_{zz}\left(\frac{\partial^2 p_{zz}}{\partial r^2}\right) + D'\frac{p_{zz}}{r}\left(\frac{\partial p_{zz}}{\partial r}\right) + D'\frac{p_{zz}}{r^2}\left(\frac{\partial^2 p_{zz}}{\partial \varphi^2}\right)\right)$$

$$\dot{T} = a_2(n'\Psi^2(p_{zz} + p_0)^2 - p_{zz})\dot{p}_{zz} + \lambda'\left(\frac{\partial^2 T}{\partial r^2}\right) + \frac{\lambda'}{r}\left(\frac{\partial T}{\partial r}\right) + \frac{\lambda'}{r^2}\left(\frac{\partial^2 T}{\partial \varphi^2}\right) \tag{18}$$

The last system of equation describes the defect and temperature evolution in sample cross section. The numerical solutions of equations (18) with surface opened for defect diffusion are presented in figure 3. We simulate one-fourth part of critical cross section. Initial condition includes three defect density fluctuations. One of them is located far from the surface, two other - on sample surface.

Figures 2a,b,c corresponds to relative high stress level. Under such loading condition we model the ordinary high cyclic fatigue. The initial high defect concentration near sample surface plays the main role and lead to the emergence of blow-up defect structures located at sample surface. The sharp increasing of defect concentration can be considered as crack initiation. Figures 2d,e,f present the corresponding temperature distributions.

Figures 3a,b,c corresponds to relatives small stress level. Under such loading condition we model we can observe completely different defect evolution. The defect fluctuation density located far from the sample surface became more dangerous from failure point of view. The loading process became longer and surface plays a stabilization role. We can observe the increasing of defect concentration and initiation blow-up structures in bulk of the sample. Figures 3d,e,f present the corresponding temperature distributions.

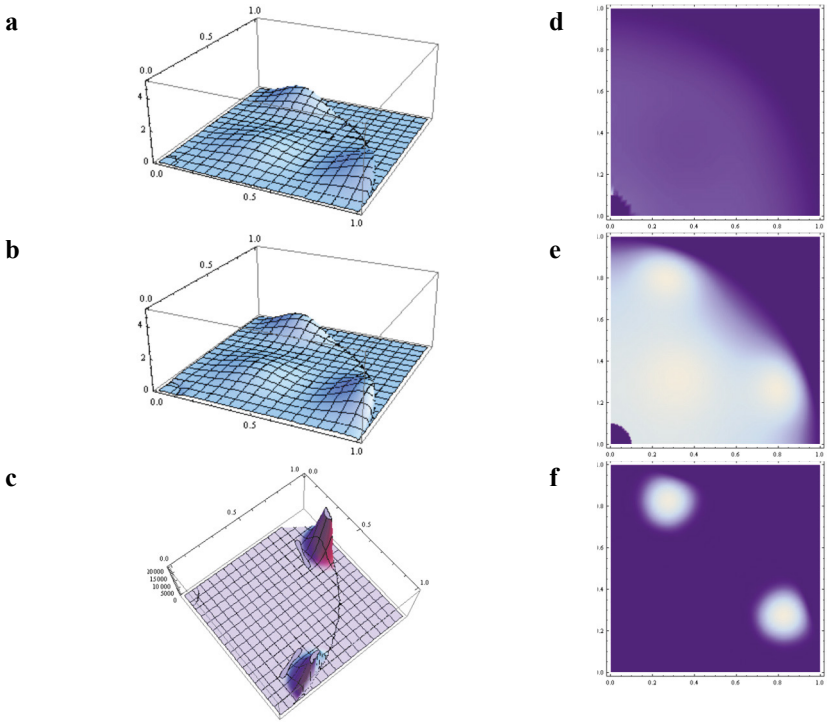

Fig. 2. a,b,c - defect induced strain evolution at different times of loading at high stress amplitude, (a) – initial defect concentration, (c) – failure initiation; d,e,f – corresponding temperature distributions.

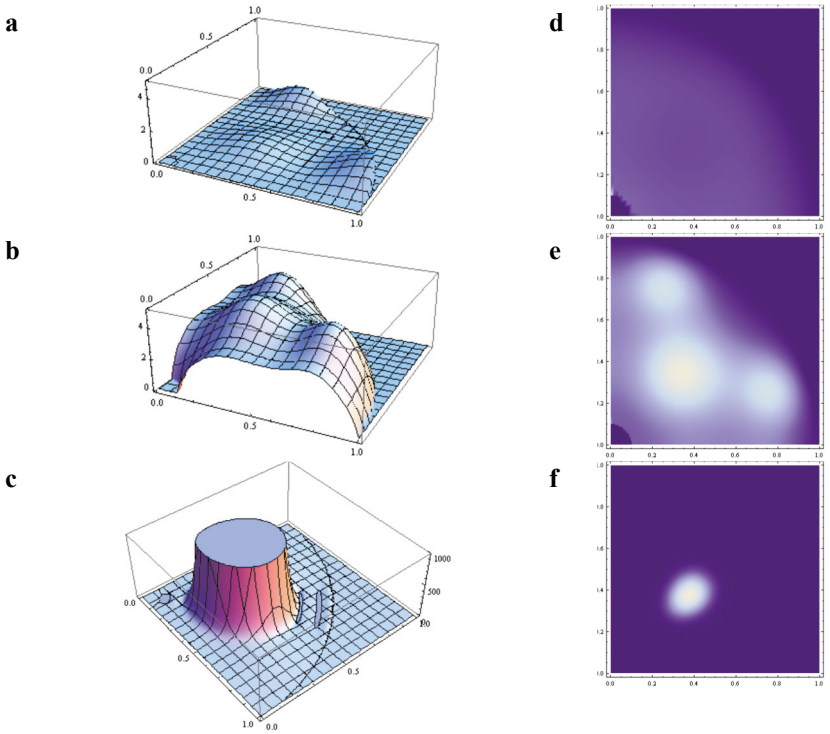

Fig. 4. a,b,c - defect induced strain evolution at different times of loading at small stress amplitude. (a) – initial defect concentration, (c) – failure initiation; d,e,f – corresponding temperature distributions.

5. Conclusion

The results of structural investigation allow us to make a following conclusion. The increase of the number of cycles under ultrasonic fatigue test leads to the sample dilatation. The dilatation can be caused by initiation of new dislocations, micro voids and cracks. The hydrostatic weighing shows that the maximum of dilatation is observed in the middle part of the iron samples.

The high initial concentration of these defects in metals and their initiation during initial stage of deformation process allows us to propose the importance of the consideration of their evolution under cyclic loading. The small size and high concentration of submicrocracks in metals, the existing of their size and orientation distributions allows us to develop a statistical description of microcrak evolution in metals under cyclic loading and introduce a new thermodynamical variable – defect induced strain. The new variable gives a natural description of thermodynamics of metals with microcracks and allows one to describe the interaction of plasticity and failure processes.

The combination of statistical description of microcrack ensemble with stochastic consideration of defect initiation process allows us to describe the effect of initial nucleus concentration of the deformation process. This model coupled with a description of nonlocal effect in the defect ensemble gives us a key parameter for the description of defect kinetics in the bulk and near specimen surface under cyclic loading.

The model illustrates the basic physical mechanisms of damage to fracture transition under fatigue loading in the bulk and near specimen surface and calculate the corresponding temperature evolution. It was shown that the stress amplitude can influence on the location of macro fatigue crack initiation. At small stress amplitude the defect induced strain reaches an equilibrium value near specimen surface due to the defect diffusion and annihilation processes. It can be considered as an infinite fatigue life but in this case there is possibility of blow-up regime of defect kinetics in the volume of the specimen. It leads to the shift of the location of the crack initiation from the surface to the volume of the specimen.

Acknowledgements

The work was funded by RFBR according to the research project No.14-01-00122, No.14-01-96005.

References

Murakami Y., Nomoto T., Ueda T., 1999. Factors influencing mechanism of superlong fatigue failure in steel. Fatigue & Fracture of Engineering Materials & Structures 22, 581-590.

Bathias C., Paris P., 2004. Gigacycle Fatigue in Mechanical Practice, Taylor & Francis, pp. 328

Zhu X., Shyam A., Jones J.W., Mayer H., Lasecki J.V., Allison J.E., 2006. Effect of microstructure and temperature on fatigue behavior of E319-T7 cast aluminum alloy in very long life cycles. International Journal of Fatigue 28, 1566-1571.

Liu X., Sun Ch., Hong Y., 2015. Effects of stress ratio on high-cycle and very-high-cycle fatigue behavior of a Ti–6Al–4V alloy. Materials Science and Engineering: A. 622, 228-235.

Mayer H., Schuller R., Karr U., Irrasch D., Fitzka M., Hahn M., Bacher-Höchst M., 2015. Cyclic torsion very high cycle fatigue of VDSiCr spring steel at different load ratios. International Journal of Fatigue 70, 322-327.

Nikitin A., Bathias C., Palin-Luc T., Shanyavskiy A., 2016. Crack path in aeronautical titanium alloy under ultrasonic torsion loading. Frattura ed Integrita Strutturale 10, 213-222.

Ranc N., Favier V., Munier B., Vales F., Thoquenne G., Lefebvre F., 2015. Thermal Response of C45 Steel in High and Very High Cycle Fatigue. Procedia Engineering 133, 265-271

Plekhov O., Naimark O., Semenova I., Polyakov A., Valiev R., 2015. Experimental study of thermodynamic and fatigue properties of submicrocrystalline titanium under high cyclic and gigacyclic fatigue regime", Proceedings of the Institution of Mechanical Engineers Part C - Journal of Mechanical Engineering Science 229, 1271-1279.

Crupi V., Epasto G., Guglielmino E., Risitano G., 2015. Thermographic method for very high cycle fatigue design in transportation engineering, Proceedings of the Institution of Mechanical Engineers Part C - Journal of Mechanical Engineering Science 229, 1260-1270.

Crupi V., Epasto G., Guglielmino E., Risitano G., 2015. Analysis of temperature and fracture surface of AISI4140 steel in very high cycle fatigue regime. Theoretical and Applied Fracture Mechanics 80, 22-30

Naimark O., 2003. Defect Induced Transitions as Mechanisms of Plasticity and Failure in Multifield Continua In "Advances in Multifield Theories of Continua with Substructure", Birkhauser Boston, Inc., pp. 75-87.

Doudard C. Calloch S., Cugy P., Galtier A., Hild F., 2005. A probabilistic two-scale model for high-cycle fatigue life predictions. Fatigue & Fracture of Engineering Materials & Structures 28, 279–288.